

Crack Modeling and Detection in Rotating System by using different FEM beam theories

Salman KH. KH. Al-Driasawi g.den84@yahoo.com

Xuan Jianping jpxuan@hust.edu.cn

Anas Hamid K. AL-jemely anasaljemely@yahoo.com

Qamar ud Din Abid abid.mech@hotmail.com

Abstract

Fault identification in the rotor system In this paper, finite element method used to model a simply support beam. A beam theories has been used in analysis to estimate the natural frequencies of beam which utilized as an indicator to presence of crack. Existence of crack in element lead to increase the flexibility of element. Moment of inertia is very sensitive to change of cross section of beam when crack is propagation, therefore the size of crack has been described in this term. Timoshenko and Euler beam theory are used for modeling and detection the crack along the length of shaft with different size and location when rotary effects and shear considered and ignored.

keywords: Fault, Identification, Crack, FEM, Timoshenko beam theory, Euler beam theory, Natural frequency.

1 Introduction

Modern industries are widely used rotating machinery and its utilized ranging from domestic appliances to power plan. One of the most faults which leads to catastrophic failure and taken wide consideration of researchers is crack of rotating shaft unless detection early. The vibration of bending and longitudinal coupling in shaft due to open crack has been studied the local flexibility matrix of the cracked shaft. The frequency equation solved and derived have done for the natural frequencies of a rotor system. it has been noticed that the natural frequencies vary with the change of crack depth.[2] Again this issue has been studied but used stationary shaft with two breathing cracks. Euler beam theory has been used for modeling rotating shaft and calculate the response with different orientations.[3] The general crack with additional slope and bending moment at crack position are used to analyzing the dynamic behavior based on harmonic motion.[4]

The harmonics 2X and 3X used to detection crack in a non-linear rotor system. The effect of crack location and size on the non-linear response are studied.[5] A new formula is presented to improve the models used by crack detection techniques. FEM is used as a model for simple beams and compared the results of this formula with the priors studies.[6] FEM used for computing the eigensystem for a cracked beam with different degree of closure. Linear elastic fracture mechanism,FEM and component mode synthesis theory are derived.[7]. A new breathing functions are identified to represent the actual breathing effect of crack on the stiffness element due to shaft weight and varying area moment of inertia for shaft during rotation. Finite element equation and harmonic balance method for response are solved and formulated.[8] A non destructive evaluation method is used to detection crack size and its location for aluminum beams experimentally. Variations in the natural frequencies and mode shapes were used as a indicator to presence of cracks in the beams.measurements of the acceleration frequency responses at a different points were taken using a dual channel frequency analyzer.[9] Different types of crack are consider in a model based identification method of transverse cracks in rotating shaft . The efficiency of this method is validated by experimental data obtained on a large rig, the identification and method and relative theory are briefly explained.[10] Fatigue crack is a common rotor faults,and it has a great potential to cause catastrophic faults in the rotating machines . Various researchers are modeled cracks with a different methodolo-

gy and investigated the dynamic of crack in the rotating system.finite element method is a proper decision for modeling a crack in the rotor shaft and analyze the dynamics behavior of rotating system.[11].

In this paper,simply support beam carrying two disks between two bearings has been modeled by using Euler and Timoshenko beam theories,also the gyroscopic effect includes in the numerical analysis,and detected the presence of crack along the shaft by monitoring the first fourth natural frequencies.

2 Numerical method

In this work,FEM used to model and analysis a simply support beam carry two disks. Two theories were used in this study to show the different between those theories'Timoshenko and Euler beam theory'.In the same technique,effect of crack is included and its effects on the natural frequency are discussed. Manly the system consists of three items which explained in the next sections.

2.1 Disk modeling

This section explain how to model disk.The kinetic energy because the rotating of disk appear in two directions translation and rotation.Set of equations below show the modeling of kinetic energy.

$$\frac{1}{2}(diskmass)(linervelocity)^2 = \frac{1}{2}m_d(\bar{u} + \dot{v}) \quad (1)$$

Now, we can expression the kinetic energy due to translation and rotational of disk.

$$\frac{1}{2}I_d(\omega_x^2 + \omega_y^2) + \frac{1}{2}I_p\omega_z^2 \quad (2)$$

rotation must be respect to the rotation axes are rotating with the disk, to do this have to use transformation matrix.[12]

$$\begin{pmatrix} \omega_x \\ \omega_y \\ \omega_z \end{pmatrix} = \begin{pmatrix} 0 \\ 0 \\ \Omega \end{pmatrix} + \begin{bmatrix} \cos \phi & \sin \phi & 0 \\ -\sin \phi & \cos \phi & 0 \\ 0 & 0 & 1 \end{bmatrix} \begin{pmatrix} \dot{\theta} \\ 0 \\ 0 \end{pmatrix} + \begin{bmatrix} \cos \phi & \sin \phi & 0 \\ -\sin \phi & \cos \phi & 0 \\ 0 & 0 & 1 \end{bmatrix} \begin{pmatrix} 1 & 0 & 0 \\ 0 & \cos \theta & \sin \theta \\ 0 & -\sin \phi & \cos \phi \end{bmatrix} \begin{pmatrix} 0 \\ \dot{\psi} \\ 0 \end{pmatrix} \quad (3)$$

and the results of multiply for this transform are

$$\begin{pmatrix} \omega_x \\ \omega_y \\ \omega_z \end{pmatrix} = \begin{pmatrix} \dot{\theta} \cos \phi + \dot{\psi} \sin \phi \cos \theta \\ -\dot{\theta} \sin \phi + \dot{\psi} \cos \phi \cos \theta \\ \Omega - \dot{\psi} \sin \theta \end{pmatrix} \quad (4)$$

To find the total kinetic energy due to translation and rotational motion for disk, equation of total kinetic energy due to translation and rotational and substitute the value of angular velocities in the equation as below

$$\begin{aligned} T_d &= \frac{1}{2}m_d(\dot{u}^2 + \dot{v}^2) + \frac{1}{2}I_d(\omega_x^2 + \omega_y^2) + \frac{1}{2}I_p\omega_z^2 \quad (5) \\ &= \frac{1}{2}m_d(\dot{u}^2 + \dot{v}^2) + \frac{1}{2}I_d(\dot{\theta}^2 + \dot{\psi} \cos^2 \theta) + \\ &\quad \frac{1}{2}I_p(\Omega^2 - 2\Omega\dot{\psi} \sin \theta + \dot{\psi}^2 \sin^2 \theta) \quad (6) \end{aligned}$$

Let us assume that θ and ψ are small, so we get

$$T_d = \frac{1}{2}m_d(\dot{u}^2 + \dot{v}^2) + \frac{1}{2}I_d(\dot{\theta}^2 + \dot{\psi}^2) + \frac{1}{2}I_p(\Omega^2 - 2\Omega\dot{\psi}\theta) \quad (7)$$

Applying lagrange's equation to get the disk mass matrix and gyroscopic matrix as in these equations 9.

$$[u, v, \theta, \psi]^T \quad (8)$$

$$c = \begin{bmatrix} m_d & 0 & 0 & 0 \\ 0 & m_d & 0 & 0 \\ 0 & 0 & I_d & 0 \\ 0 & 0 & 0 & I_d \end{bmatrix} \begin{pmatrix} \ddot{u} \\ \ddot{v} \\ \ddot{\theta} \\ \ddot{\psi} \end{pmatrix} +$$

$$\Omega \begin{bmatrix} 0 & 0 & 0 & 0 \\ 0 & 0 & 0 & 0 \\ 0 & 0 & 0 & I_p \\ 0 & 0 & -I_p & 0 \end{bmatrix} \begin{Bmatrix} \dot{u} \\ \dot{v} \\ \dot{\theta} \\ \dot{\psi} \end{Bmatrix} \quad (9)$$

The disk element mass matrix is

$$M_e = \begin{bmatrix} m_d & 0 & 0 & 0 \\ 0 & m_d & 0 & 0 \\ 0 & 0 & I_d & 0 \\ 0 & 0 & 0 & I_d \end{bmatrix} \quad (10)$$

Gyroscopic matrix is

$$G_e = \begin{bmatrix} 0 & 0 & 0 & 0 \\ 0 & 0 & 0 & 0 \\ 0 & 0 & 0 & I_p \\ 0 & 0 & -I_p & 0 \end{bmatrix} \quad (11)$$

3 Beam Theories

There are list of beam theories used to model shafts and beams, in this research focus on two theories to model a rotor system and identical the effect of faults on the dynamics characteristic like natural frequency, mode shapes and their amplitude. Figure(1) show the different between these theories.

3.1 Euler Theory

In modeling and analysis with classical theory unconsider shear and rotary inertia effects. Stiffness matrix and mass matrix are derived from strain energy and kinetic energy. [13]

$$U_e = \frac{1}{2} \int_0^{\ell_e} E_e I_e (\xi) \left(\frac{\partial^2 u_e(\xi, t)}{\partial \xi^2} \right)^2 d\xi \quad (12)$$

where :

E_e Young's modulus.

I_e second moment of area.

ℓ_e length of element.

Let us assume the cross section does not vary along the element equation above it becomes

$$U_e = \frac{1}{2} E_e I_e \int_0^{\ell_e} \left(\frac{\partial^2 u_e(\xi, t)}{\partial \xi^2} \right)^2 d\xi \quad (13)$$

Approximation is used to the strain energy of beam

$$U_e = \frac{1}{2} \begin{Bmatrix} u_{e1}(t) \\ \psi_{e1}(t) \\ u_{e2}(t) \\ \psi_{e2}(t) \end{Bmatrix}^T \begin{bmatrix} k_{11} & k_{12} & k_{13} & k_{14} \\ k_{21} & k_{22} & k_{23} & k_{24} \\ k_{31} & k_{32} & k_{33} & k_{34} \\ k_{41} & k_{42} & k_{43} & k_{44} \end{bmatrix} \begin{Bmatrix} u_{e1}(t) \\ \psi_{e1}(t) \\ u_{e2}(t) \\ \psi_{e2}(t) \end{Bmatrix} \quad (14)$$

where:

k : stiffness of element.

Evaluate strain energy of the element have to calculate the stiffness matrix for elements, equation below used to evaluate it.

$$k_{ij} = E_e I_e \int_0^{\ell_e} \frac{\partial^2 N_{ei}}{\partial \xi^2} \frac{\partial^2 N_{ej}}{\partial \xi^2} \quad (15)$$

$$k_e = \begin{bmatrix} k_{11} & k_{12} & k_{13} & k_{14} \\ k_{21} & k_{22} & k_{23} & k_{24} \\ k_{31} & k_{32} & k_{33} & k_{34} \\ k_{41} & k_{42} & k_{43} & k_{44} \end{bmatrix}$$

$$= \frac{E_e I_e}{\ell^3} \begin{bmatrix} 12 & 6\ell_e & -12 & 6\ell_e \\ 6\ell_e & 4\ell_e^2 & -6\ell_e & 2\ell_e^2 \\ -12 & -6\ell_e & 12 & -6\ell_e \\ 6\ell_e & 2\ell_e^2 & -6\ell_e & 4\ell_e^2 \end{bmatrix} \quad (16)$$

Strain energy equation is

$$U_e = X^T K_e X \quad (17)$$

Where X is a vector 4×1 and represent the nodal displacement.

Mass element matrix derived from kinetic energy equation.

$$T_e = \frac{1}{2} \int_0^{\ell_e} \rho_e A_e(\xi) \dot{u}_e^2(\xi, \tau) d\xi \quad (18)$$

where:

ρ_e Density of the material.

A_e Cross section area of the beam.

$$T_e = \frac{1}{2} \begin{Bmatrix} \dot{u}_{e1}(t) \\ \dot{\psi}_{e1}(t) \\ \dot{u}_{e2}(t) \\ \dot{\psi}_{e2}(t) \end{Bmatrix}^T \begin{bmatrix} m_{11} & m_{12} & m_{13} & m_{14} \\ m_{21} & m_{22} & m_{23} & m_{24} \\ m_{31} & m_{32} & m_{33} & m_{34} \\ m_{41} & m_{42} & m_{43} & m_{44} \end{bmatrix} \begin{Bmatrix} \dot{u}_{e1}(t) \\ \dot{\psi}_{e1}(t) \\ \dot{u}_{e2}(t) \\ \dot{\psi}_{e2}(t) \end{Bmatrix} \quad (19)$$

Mass matrix for a uniform cross section of beam is evaluated by the eq.bellow

$$m_{ij} = \rho_e A_e \int_0^{\ell_e} N_{ei}(\xi) N_{ej}(\xi) d\xi \quad (20)$$

Computing the integrals of all elements of mass matrix in the eq. gives

$$M_e = \begin{bmatrix} m_{11} & m_{12} & m_{13} & m_{14} \\ m_{21} & m_{22} & m_{23} & m_{24} \\ m_{31} & m_{32} & m_{33} & m_{34} \\ m_{41} & m_{42} & m_{43} & m_{44} \end{bmatrix} = \frac{\rho_e A_e \ell_e}{420} \begin{bmatrix} 156 & 22\ell_e & 54 & -13\ell_e \\ 22\ell_e & 4\ell_e^2 & 13\ell_e & -3\ell_e^2 \\ 54 & 13\ell_e & 156 & -22\ell_e \\ -13\ell_e & -3\ell_e^2 & -22\ell_e & 4\ell_e^2 \end{bmatrix} \quad (21)$$

Final strain energy equation is

$$T_e = \dot{X}^T M_e X \quad (22)$$

where, \dot{X} is a vector 4×1 and represent the time derivative of nodal displacement

3.2 Timoshenko Beam theory

In this theory, the effects of shear and rotary inertia are considered. The cross section of beam remain perpendicular with a small difference between the plain of beam cross section and the normal to the beam center line as in fig. Therefore, the angle of beam cross section it will becomes. [14]

$$\psi_e(\xi, \tau) = \frac{\partial u_e(\xi, \tau)}{\partial \xi} + \beta_e(\xi, \tau) \quad (23)$$

$$T_e = \frac{1}{2} \begin{Bmatrix} \dot{u}_{e1}(t) \\ \dot{\psi}_{e1}(t) \\ \dot{u}_{e2}(t) \\ \dot{\psi}_{e2}(t) \end{Bmatrix}^T \begin{bmatrix} m_{11} & m_{12} & m_{13} & m_{14} \\ m_{21} & m_{22} & m_{23} & m_{24} \\ m_{31} & m_{32} & m_{33} & m_{34} \\ m_{41} & m_{42} & m_{43} & m_{44} \end{bmatrix} \begin{Bmatrix} \dot{u}_{e1}(t) \\ \dot{\psi}_{e1}(t) \\ \dot{u}_{e2}(t) \\ \dot{\psi}_{e2}(t) \end{Bmatrix} \quad (24)$$

write the equation in this form mass of element equal to

$$m_{ij} = \rho_e A_e \int_0^{\ell_e} N_{ei}(\xi) N_{ej}(\xi) d\xi \quad (25)$$

$$+ \rho_e A_e \int_0^{\ell_e} \left(\frac{\phi_e \ell_e^2}{12} N_{ei}'''(\xi) + N_{ei}'(\xi) \right) \left(\frac{\phi_e \ell_e^2}{12} N_{ej}'''(\xi) + N_{ej}'(\xi) \right) d\xi \quad (26)$$

the equivalent mass matrix is

$$M_e = \frac{\rho_e A_e \ell_e}{840(1 + \phi_e)^2} \begin{bmatrix} m_1 & m_2 & m_3 & m_4 \\ m_2 & m_5 & -m_4 & m_6 \\ m_3 & -m_4 & m_1 & -m_2 \\ m_4 & m_6 & -m_2 & m_5 \end{bmatrix} \quad (27)$$

$$+ \frac{\rho_e I_e}{30(1 + \phi_e)^2 \ell_e} \begin{bmatrix} m_7 & m_8 & -m_7 & m_8 \\ m_8 & m_9 & -m_8 & m_{10} \\ -m_7 & -m_8 & m_7 & -m_8 \\ m_8 & m_{10} & -m_8 & m_9 \end{bmatrix}$$

where :

$$m_1 = 312 + 588\phi_e + 280\phi_e^2;$$

$$m_2 = \ell_e(44 + 77\phi_e + 35\phi_e^2);$$

$$m_3 = 108 + 252\phi_e + 140\phi_e^2;$$

$$m_4 = -\ell_e(26 + 63\phi_e + 35\phi_e^2);$$

$$m_5 = \ell_e^2(8 + 14\phi_e + 7\phi_e^2);$$

$$m_6 = -\ell_e(6 + 14\phi_e + 7\phi_e^2);$$

$$m_7 = 36;$$

$$m_8 = \ell_e(3 - 15\phi_e)$$

$$m_9 = \ell_e^2(4 + 5\phi_e + 10\phi_e^2);$$

$$m_{10} = \ell_e^2(-1 - 5\phi_e + 5\phi_e^2)$$

$$T_{Ge} = -2\rho_e I_e \Omega \int_0^{\ell_e} \dot{\psi}_e(\xi, \tau) \theta_e(\xi, \tau) d\xi \quad (28)$$

Same equations of shape function are used to derive Gyroscopic matrix

$$G_e = \frac{\rho_e I_e}{15\ell_e} \begin{bmatrix} 36 & -3\ell_e & -36 & -3\ell_e \\ 3\ell_e & -4\ell_e^2 & -3\ell_e & \ell_e^2 \\ -36 & 3\ell_e & 36 & 3\ell_e \\ 3\ell_e & \ell_e^2 & -3\ell_e & -4\ell_e^2 \end{bmatrix} \quad (29)$$

3.3 Gyroscopic matrix with including shear and rotary effect

Gyroscopic matrix if the rotary inertia and shear effect are consider it will become :

$$G_e = \frac{\rho_e I_e}{15\ell_e(1 + \phi)^2} \begin{bmatrix} n_1 & -n_2 & -n_1 & -n_2 \\ n_2 & -n_3 & -n_2 & -n_4 \\ -n_1 & n_2 & n_1 & n_2 \\ n_2 & -n_4 & -n_2 & -n_3 \end{bmatrix} \quad (30)$$

Where :

$$n_1 = 36.$$

$$n_2 = (3 - 15\phi_e)\ell_e.$$

$$n_3 = (4 + 5\phi_e + 10\phi_e^2)\ell_e^2.$$

$$n_4 = (-1 - 5\phi_e + 5\phi_e^2)\ell_e^2.$$

4 Crack modeling

To model presence of crack in the beam by using FEM, generally, there are two method as shown in the figures 1-2 Crack model as a reduction in the beam geometry or substitute the crack location by a spring with stiffness value less than the stiffness of the

beam. In overall,when the crack presence in the beam,the stiffness will reduced because of that dynamic characteristics will effected,therefore,the natural frequency used as an indicator to presence of crack.

$$K_{crack} = K_{uncrack} - K_{crack} \quad (31)$$

The final equation used to analyse the model and calculate the natural frequency is :

$$M\ddot{X} + [C + G]\dot{X} + KX = F(x) \quad (32)$$

5 Result of crack effect on the natural frequency

5.1 Crack location effect

Results of crack location and size effect are shown in the Figures [3 -6],the model properties and geometry were as follow; beam length=0.4m,beam diameter 0.03m,disk diameter 0.05m,disk location at third and seventh element. Figure [3] shown the effect of crack location the first natural frequency which showed the effect decay near the support,while increase at the middle of beam. Figure[4] second natural frequency mostly effected when the crack located at third element whilst the effect decrease gradually when the crack moved to element number eight. Figure [5] shown that,the effect mostly effected when locate at third and seven elements where as decay at element eight to the end of beam. The effect decreasing at the middle of beam,that is because of existence of nodal point at this point. Figure [6] maximum effect are when the crack located

at fourth and seventh element and decrease at sixth element. Crack effect on the natural frequencies are exhibits same behavior for both theories except that,value of natural frequencies used Euler Beam theory higher than Timoshenko beam theory.

5.2 Crack size effect

In Figures [7-10]the effect of crack size on the natural frequencies,Figure[7]show the crack size effect on the 1st natural frequency which showed that the value decrease as the size increased. The effect is less when the crack located at the first three elements and maximum when located in the middle of beam. On the other hand,when located at the last three elements the effect decrease gradually. In Figure[8] shown the 2nd natural frequency,which shown that the effect become maximum when the crack located at third element and vanished at the last third element. Figure[9]show 3rd natural frequency,which effected mostly when the crack located at seventh element and vanished when located at first,eight,ninth and tenth elements. The behaviour are not proportionally with crack location, while proportionally with the crack size. Figure[10] show fourth natural frequency,which mostly effected when the crack located at fourth element,where as vanished when located at the first and last three elements for all size.

5.3 Identification technique

The result of crack size and location effect are used as a data base to generate a 3D-

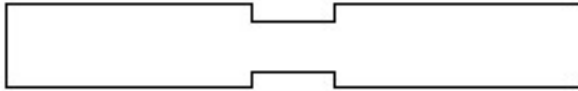


Figure 1: crack modelling by using stiffness reduction

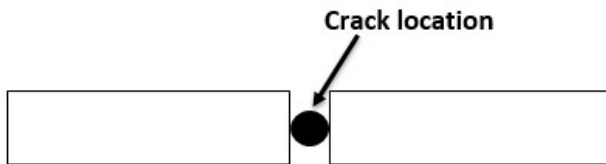


Figure 2: crack modelling by using stiffness join

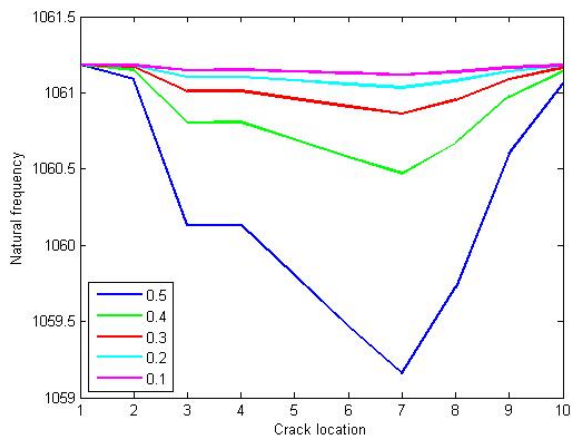


Figure 3: Crack location effect on the first natural frequency

Figure 4: Crack location effect on the second natural frequency

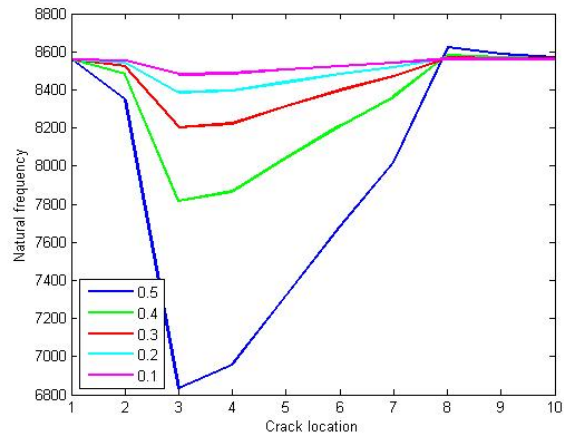
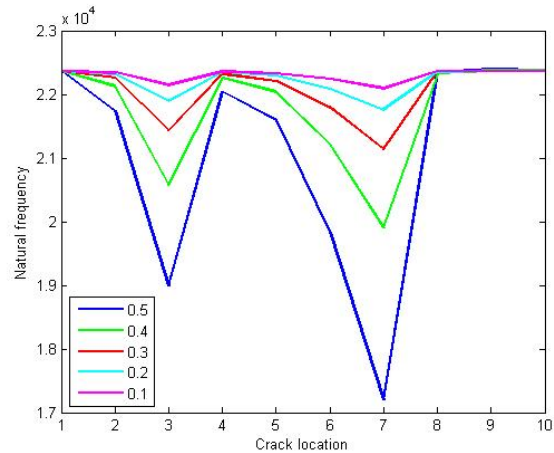


Figure 5: Crack location effect on the third natural frequency



plot for the first fourth natural frequencies to normalized the natural frequencies as in the Figures[11-14]. Then use contour plot for any three natural frequencies as function of crack size and location on the same plot axis,the

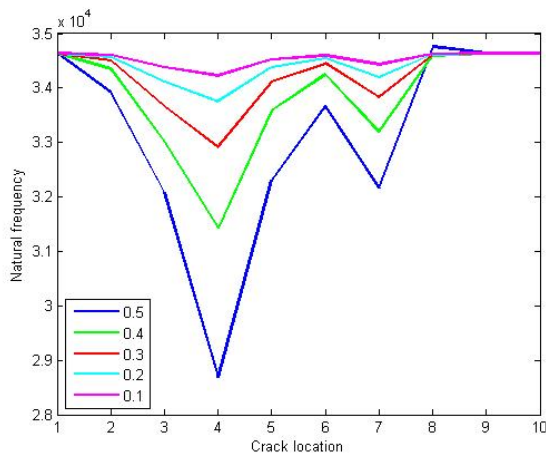


Figure 6: Crack location effect on the fourth natural frequency

intersect of any three points is represent the values of crack size and location.

6 Conclusion

Rotor is an important part in the rotating machine, therefore it needs more aware especially during the operation, detection fault in the rotor earlier easier than maintenance when it failures, numerates faults and numerates detection method. One of the most fault which lead to catastrophic failures unless detection earlier is crack. FEM, Timoshenko and Euler beam theory, have been investigated and used in modeling of rotating beam carried two disk, dynamic characteristic for healthy beam has been calculated and include crack with a difference size and location, the different between the dynamic behaviour of beam used as an indicator to presence of crack in the beam. Result of natural frequen-

cies with different size and location used as a data base for identification technique to detection crack size and location in the beam. The result of two theories were accurate and acceptable, FEM is a good tool for modelling a rotor system and suitable to insert a fault in the modeling.

7 Acknowledgement

We would express our sincere thanks to my supervisor Prof. Xuan Jianping for his suggestion and guidance during study period.

References

- [1] Dimarogonas, Andrew D. "Vibration of cracked structures: a state of the art review." *Engineering fracture mechanics* 55, no. 5 (1996): 831-857.
- [2] Papadopoulos, C. A., and A. D. Dimarogonas. "Coupled longitudinal and bending vibrations of a rotating shaft with an open crack." *Journal of sound and vibration* 117, no. 1 (1987): 81-93.
- [3] Chasalevris, A. C., and C. A. Papadopoulos. "Coupled horizontal and vertical bending vibrations of a stationary shaft with two cracks." *Journal of Sound and Vibration* 309, no. 3 (2008): 507-528.
- [4] Jun, Oh Sung. "Dynamic behavior analysis of cracked rotor based on harmonic motion." *Mechanical Systems and Signal Processing* 30 (2012): 186-203.

- [5] Jean-Jacques Sinou. Detection of cracks in rotor based on the 2X and 3X superharmonic frequency components and the crack-unbalance interactions. *Communications in Nonlinear Science and Numerical Simulation*, Elsevier, 2008, 13, pp.2024-2040.
- [6] Ugurcan Eroglu , Ekrem Tufekci , EXACT SOLUTION BASED FINITE ELEMENT FORMULATION OF CRACKED BEAMS FOR CRACK DETECTION, *International Journal of Solids and Structures* (2016), doi: 10.1016/j.ijsolstr.2016.06.005
- [7] Kisa, M., and J. Brandon. "The effects of closure of cracks on the dynamics of a cracked cantilever beam." *Journal of Sound and Vibration* 238, no. 1 (2000): 1-18.
- [8] Al-Shudeifat, Mohammad A., and Eric A. Butcher. "New breathing functions for the transverse breathing crack of the cracked rotor system: approach for critical and subcritical harmonic analysis." *Journal of Sound and Vibration* 330, no. 3 (2011): 526-544.
- [9] Owolabi, G. M., A. S. J. Swamidas, and R. Seshadri. "Crack detection in beams using changes in frequencies and amplitudes of frequency response functions." *Journal of sound and vibration* 265, no. 1 (2003): 1-22.
- [10] Pennacchi, Paolo, Nicolo Bachschmid, and Andrea Vania. "A model-based identification method of transverse cracks in rotating shafts suitable for industrial machines." *Mechanical Systems and Signal Processing* 20, no. 8 (2006): 2112-2147.
- [11] Kumar, Chandan, and Vikas Rastogi. "A brief review on dynamics of a cracked rotor." *International Journal of Rotating Machinery* 2009 (2010).
- [12] AL-Shudeifat, Mohammad A. "On the finite element modeling of the asymmetric cracked rotor." *Journal of Sound and Vibration* 332, no. 11 (2013): 2795-2807.
- [13] Han, Seon M., Haym Benaroya, and Timothy Wei. "Dynamics of transversely vibrating beams using four engineering theories." *Journal of sound and vibration* 225, no. 5 (1999): 935-988.
- [14] Genta, Giancarlo. *Dynamics of rotating systems*. Springer Science , Business Media, 2007.

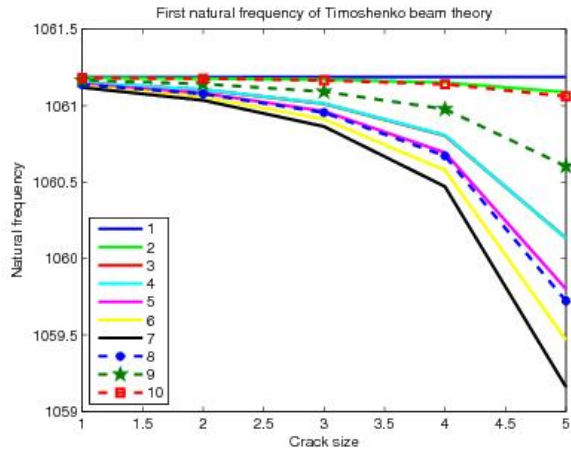


Figure 7: Crack size effect on the first natural frequency

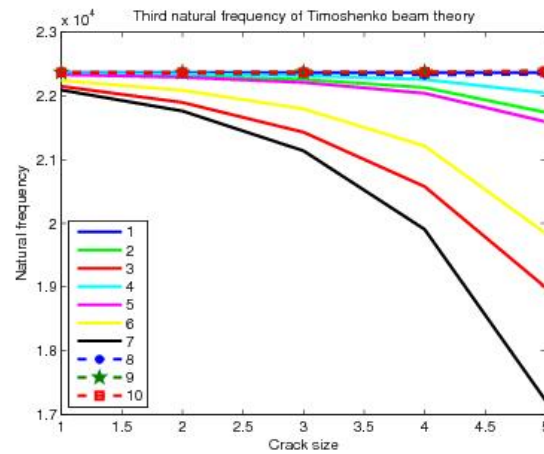


Figure 9: Crack size effect on the third natural frequency

Figure 8: Crack size effect on the second natural frequency

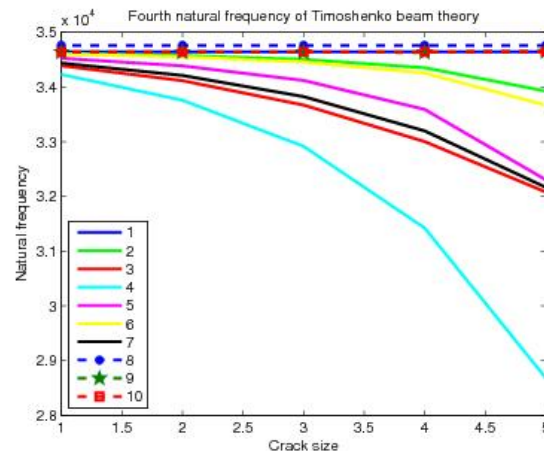
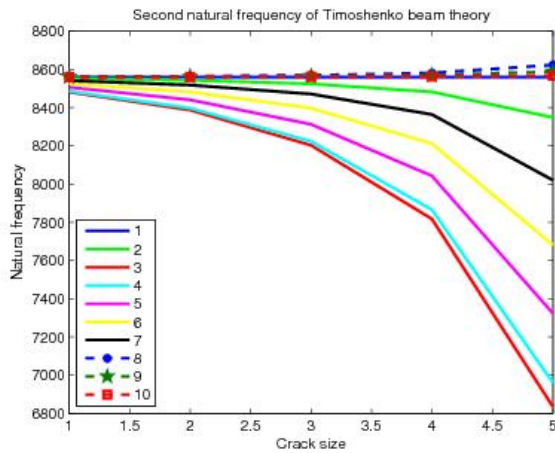


Figure 10: Crack size effect on the fourth natural frequency

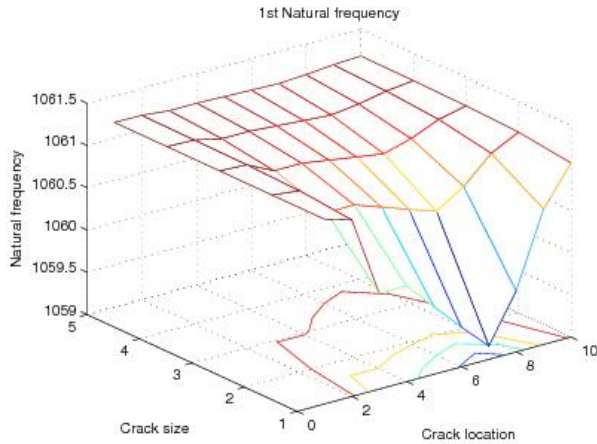


Figure 11: 3D-plot for the first natural frequency as a function of crack size and location

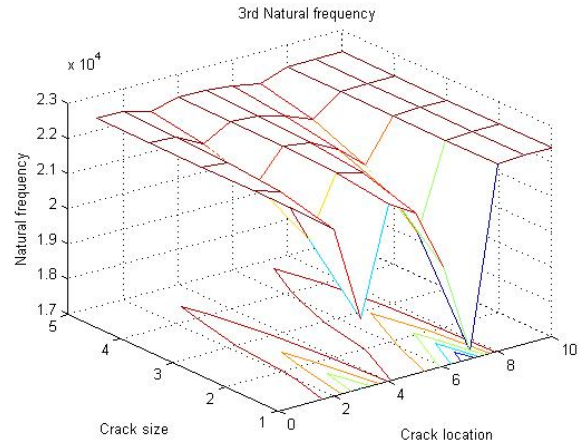


Figure 13: 3D-plot for the third natural frequency as a function of crack size and location

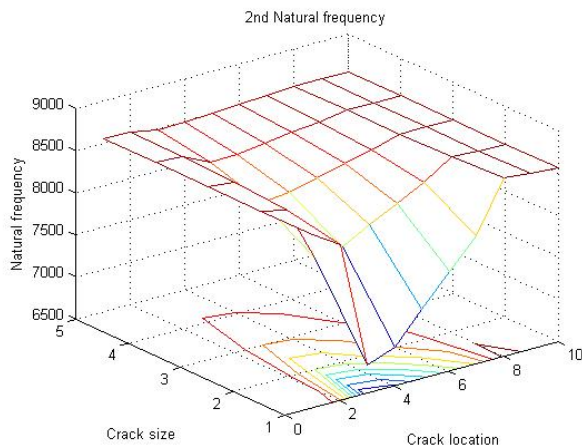


Figure 12: 3D-plot for the second natural frequency as a function of crack size and location

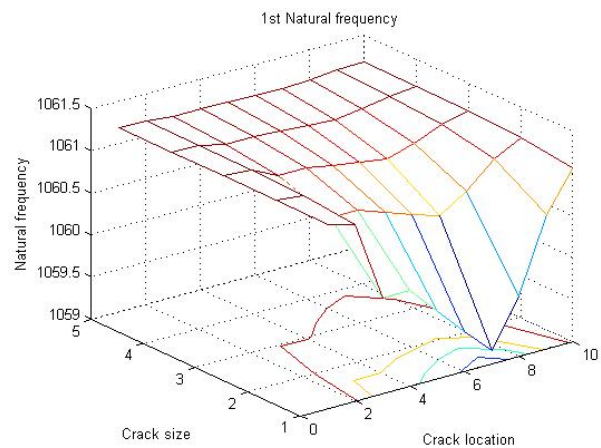


Figure 14: 3D-plot for the fourth natural frequency as a function of crack size and location